Received: *March 8, 2001*, Accepted: *May 30, 2001*
Revised: *May 28, 2001*

Towards an accurate calculation of the neutralino relic density

Takeshi Nihei
Department of Physics, Lancaster University, Lancaster LA1 4YB, England
E-mail: t.nihei@lancaster.ac.uk

Leszek Roszkowski
TH Division, CERN, CH-1211 Geneva 23, Switzerland and
Department of Physics, Lancaster University, Lancaster LA1 4YB, England
E-mail: Leszek.Roszkowski@cern.ch

Roberto Ruiz de Austri
Department of Physics, Lancaster University, Lancaster LA1 4YB, England
E-mail: r.ruizdeaustri@lancaster.ac.uk

Abstract: We re-analyze the neutralino relic density in the minimal supersymmetric standard model. We use exact expressions for the neutralino annihilation cross section into all tree-level final states, including all contributions and interference terms. We demonstrate that several final states may give comparable contributions to the relic density, including the gauge-Higgs and Higgs-Higgs boson channels. This illustrates the importance of performing a complete calculation. We consistently compare the exact results with those of the usual expansion method. We confirm that the expansion gives highly inaccurate results very near resonances and new thresholds and show that very far from such cases the discrepancy is typically only of the order of a few per cent. However, we demonstrate that, near the pseudoscalar Higgs resonance, the expansion can give a sizeable error (of more than 10%) over a significant range of the neutralino mass which can be as large as several tens of GeV. We also perform several related checks and comparisons. In particular, we show that the often employed approximate iterative procedure of computing the neutralino freeze-out temperature gives generally very accurate results, except in the case when the expansion method is used in the vicinity of resonances and thresholds.

Keywords: Supersymmetric Effective Theories, Cosmology of Theories beyond the SM, Dark Matter.

Contents

1. **Introduction** **1**

2. **Calculation of the relic density** **4**

3. **Analytic results** **7**

4. **Numerical results** **9**

5. **Conclusions** **16**

A. **Auxiliary formulae** **17**

1. Introduction

One of the most exciting unresolved issues in particle physics and cosmology is the nature of dark matter (DM) in the Universe. Cosmological and astronomical observations have over the years put significant restrictions on its properties. In particular, it is widely expected that a hypothetical candidate should be in the form of cold DM (CDM), while a combination of several measurements has narrowed the range of its relic abundance to

$$0.1 \lesssim \Omega_{\rm CDM} h^2 \lesssim 0.3\,, \tag{1.1}$$

where $\Omega_{\rm CDM}$ is the ratio of the CDM relic density to the critical density and $h \approx 0.7$ is a parameter in the Hubble constant $H_0 = 100\,h\,\mathrm{km/sec/Mpc}$ [1]. Constraints from the Big Bang Nucleosynthesis [2] and, recently, from observations of the cosmic microwave background radiation [3, 4] have strongly restricted the abundance of baryonic DM; for example, ref. [5] quotes the range $\Omega_b h^2 = 0.02 \pm 0.002$. Therefore most of the DM in the Universe is expected to be non-baryonic.

From a particle physics point of view, CDM is most naturally made of some weakly interacting (stable) massive particles (WIMPs). Supersymmetry (SUSY) [6], which over the years has emerged as a leading candidate for new physics beyond the Standard Model (SM), predicts that, in the presence of R-parity, the lightest supersymmetric particle (LSP) is stable. This alone makes the LSP an interesting candidate for a WIMP and DM in the Universe.

A SUSY candidate for the LSP WIMP is by no means unique. In models coupled to gravity there exists the gravitino, the SUSY partner of the graviton. The gravitino has long been known to be a potential candidate for DM, although it generically suffers from a well-known "gravitino problem" [7]. In SUSY models that incorporate the Peccei-Quinn solution to the strong CP problem, there exists the axino, the fermionic partner of the axion. The axino has recently been shown to be an attractive and well-motivated alternative candidate for the LSP and CDM [8]. A number of more speculative possibilities, stemming from, for example, string theories, have also been proposed. However, in some sense the simplest choice is to consider one of the superpartners of the SM particles as a potential LSP. Among these, the lightest neutralino χ stands out as probably the most natural and attractive candidate for the LSP and DM [9, 10].[1] In this paper we will focus on this case.

In order to be able to perform a reliable comparison between theoretical predictions and improving measurements of the CDM relic abundance and limits from underground DM searches, a precise calculation of the relic density becomes necessary. The constraint (1.1) is known to often provide a strong restriction on allowed combinations of SUSY masses and couplings. For example, in the minimal supergravity model (also dubbed CMSSM) the condition $\Omega_\chi h^2 < 0.3$ provides a strong upper bound of a few hundred GeV on the masses of gauginos and scalars over an overwhelming fraction of the parameter space [12, 13]. When combined with recent LEP and other data, the remaining CMSSM parameter space becomes highly restricted [14]. In the future, the range (1.1) is expected to be significantly narrowed by MAP and Planck, which in turn will lead to even stronger constraints on allowed combinations of SUSY masses and couplings.

One of the key steps in computing the relic density of the neutralino involves calculating the thermal average of its annihilation cross section times the relative velocity. This calculation is technically rather involved and, therefore, in most of the literature, approximate methods have been used. These methods are based on expanding the thermal average in powers of $x \equiv T/m_\chi$, where T is the temperature of the thermal bath and m_χ is the neutralino mass. One usually computes only the first two terms of the expansion. It has been well known that the expansion fails badly near s-channel resonances [15]–[18] and near new final-state thresholds [15, 16]. In particular, it was emphasized in ref. [17] that, owing to the very narrow width of the lightest SUSY Higgs boson h, very close to the h-resonance the error can be as large as a few orders of magnitude. However, even though the usual expansion is generally expected to be accurate enough further away from resonances and thresholds, no detailed study of this point has yet been done.

A general formalism for computing the thermal average precisely was derived in refs. [16, 19]. The thermal average can be obtained by performing a single integration over the cross section. The cross sections for the neutralino pair-annihilation into the SM fermion-pair ($f\bar{f}$) and the lightest Higgs-boson pair (hh) final states were

[1] For a comprehensive review, see, ref. [11].

JHEP05(2001)063

given in ref. [18], and for the WW and ZZ final states in ref. [20]. The annihilation into $f\bar{f}$ is often most important. However, as we will re-emphasize, other final states can also play a considerable role, depending on the model.

In this paper, we carry out a consistent re-analysis and comparison of the neutralino's relic abundance. First, we carefully examine all the dominant and subdominant channels of the neutralino pair-annihilation into all 2-body final states. Next, we consistently compare $\Omega_\chi h^2$ computed using the approximate expansion method with that using exact results for the neutralino pair-annihilation cross section. Finally, we perform some related checks and comparisons. In particular, we examine the accuracy of a well-known, and widely-used, iterative procedure for solving the Boltzmann equation. We work within the framework of the minimal supersymmetric standard model (MSSM).

As a basis for our analysis, we use a full set of exact analytic expressions for the cross section of the neutralino pair-annihilation in the MSSM which will appear elsewhere [21]. In deriving them we have made no simplifying assumptions about the degeneracy of the left- and right-sfermion masses, and we included all tree-level final states and all intermediate states. We have kept finite widths in s-channel resonances. While interference terms and usually sub-dominant channels are sometimes neglected in the literature, in some cases they may give significant contributions. In particular, the channels involving gauge-Higgs boson may in some cases be sizeable or even dominant. One example where this is the case is the $W^\pm H^\mp$ final state, and in this paper we give expressions for the cross section for the chargino exchange contribution.

Next, we perform a consistent comparison of the relic abundance computed using our exact formulae with the one obtained using our expansion formulae. To this end, we expand the exact expressions in powers of x and keep, as usual, the first two terms. So far, no such detailed and consistent analysis has been presented in the literature in the case of the MSSM. In particular, ref. [17] only dealt with the h and Z-resonances, neglected interference terms and used expansion expressions for the sfermion exchange. In ref. [18] a more rigorous comparison was made but only in the context of the rather constrained minimal supergravity scheme and only relatively close to the h and Z-resonances.

We confirm that the expansion gives highly inaccurate results near resonances and new thresholds. We also show that very far from such cases the error is typically rather small, of the order of a few per cent. However, we find that, because of the existence of several resonances (Z and the Higgs bosons), the expansion produces large errors, compared to an exact treatment, over a sizeable range of m_χ which can be as large as several tens of GeV. We therefore conclude that the widely used method of expansion may lead to substantial errors in a significant fraction of the neutralino mass which is typically expected not to much exceed $\sim 200\,\mathrm{GeV}$ by various naturalness criteria [23, 24].

As a check of our exact cross sections, we have performed a numerical comparison of all the partial cross sections with the results obtained using the recently released code DarkSusy [22]. We have found, for the same values of input parameters, an impressive agreement, at the level of a few per cent, for all the annihilation channels, which we find reassuring. Finally, in the current version of our code we have used a popular approximate iterative method of determining the freeze-out point. We have examined the accuracy of the procedure and compared our results with the ones obtained using DarkSusy. We have found that the method in general works very well when both exact and expansion methods are used, except in the latter case near resonances and thresholds where it may even break down. The iterative procedure can be safely applied in such special cases, provided exact expressions for the cross section are used and much care is paid to properly integrating the thermal average numerically.

The paper is organized as follows. In section 2 we briefly review the formalism and methods used in computing the neutralino relic density. In section 3 we list all the 2-body final states and provide an example of the partial cross section for the $W^{\pm}H^{\mp}$ final state which is often sizeable. Finally, we present results of our detailed numerical analysis in section 4.

2. Calculation of the relic density

The relic abundance of some stable species χ is given by $\Omega_\chi \equiv \rho_\chi/\rho_{\rm crit}$, where ρ_χ is the relic's (mass) density and $\rho_{\rm crit} \equiv 3H_0^2/8\pi G = 1.9\times 10^{-29}\,(h^2)\,\mathrm{g/cm^3}$ is the critical density. It can be computed by solving the Boltzmann equation, which describes the time evolution of the number density n_χ in the expanding Universe,[2]

$$\frac{dn_\chi}{dt} = -3Hn_\chi - \langle\sigma v_{\rm M\o l}\rangle\left(n_\chi^2 - (n_\chi^{\rm eq})^2\right), \tag{2.1}$$

where $n_\chi^{\rm eq}$ is the number density that the species would have in thermal equilibrium, $H(T)$ is the Hubble expansion rate, $\sigma(\chi\chi \to \text{all})$ denotes the cross section of the species annihilation into ordinary particles, $v_{\rm M\o l}$ is a so-called Møller velocity [16] which is the relative velocity of the annihilating particles, and $\langle\sigma v_{\rm M\o l}\rangle$ represents the thermal average of $\sigma v_{\rm M\o l}$ which will be given below. In the early Universe, the species χ were initially in thermal equilibrium, $n_\chi = n_\chi^{\rm eq}$. When their typical interaction rate Γ_χ became less than the Hubble parameter, $\Gamma_\chi \lesssim H$, the annihilation process froze out. Since then their number in a co-moving volume has remained basically constant.

In order to calculate the relic density precisely enough, one has to consider the following ingredients: (i) compute all the contributions to the annihilation cross section, (ii) use an exact formula for the thermal average, (iii) rigorously solve the Boltzmann equation, and (iv) include co-annihilation. (This becomes important when the mass

[2]For a review of calculations of the relic density, see, e.g., refs. [11, 25].

of the next LSP is nearly degenerate with the LSP mass [15, 26, 27, 28].) In this work, we will concentrate on points (i) and (ii) but will also examine to some extent point (iii). In particular, we will compare the usually used expansion formulae with the exact ones. We will not consider here the effect of co-annihilation.

An often used, approximate, although in general quite accurate (see later), solution to the Boltzmann equation is based on solving iteratively the equation

$$x_f^{-1} = \ln\left(\frac{m_\chi}{2\pi^3}\sqrt{\frac{45}{2g_* G_N}}\langle\sigma v_{\text{Møl}}\rangle(x_f)\,x_f^{1/2}\right), \tag{2.2}$$

where g_* represents the effective number of degrees of freedom at freeze-out ($\sqrt{g_*} \simeq 9$) and G_N is the Newton constant. Typically one finds that the freeze-out point $x_f \equiv T_f/m_\chi$ is roughly given by $1/20$. The relic density $\rho_\chi = m_\chi n_\chi$ at present is given by

$$\rho_\chi = \frac{1.66}{M_{\text{Pl}}}\left(\frac{T_\chi}{T_\gamma}\right)^3 T_\gamma^3\sqrt{g_*}\frac{1}{J(x_f)}, \tag{2.3}$$

where M_{Pl} denotes the Planck mass, T_χ and T_γ are the present temperatures of the neutralino and the photon, respectively. The suppression factor $(T_\chi/T_\gamma)^3 \approx 1/20$ follows from entropy conservation in a comoving volume [29]. Finally, $J(x_f)$ is given by

$$J(x_f) \equiv \int_0^{x_f} dx\langle\sigma v_{\text{Møl}}\rangle(x), \tag{2.4}$$

where $x = T/m_\chi$, as defined earlier.

Below we will concentrate on computing $J(x_f)$ and in particular on the thermally averaged annihilation cross section times velocity $\langle\sigma v_{\text{Møl}}\rangle$. A proper definition which includes separate thermal baths for both annihilating particles is given by [19, 16]

$$\langle\sigma v_{\text{Møl}}\rangle(T) = \frac{\int d^3p_1 d^3p_2\,\sigma v_{\text{Møl}}\,e^{-E_1/T}e^{-E_2/T}}{\int d^3p_1 d^3p_2\,e^{-E_1/T}e^{-E_2/T}} \tag{2.5}$$

where $p_1 = (E_1, \mathbf{p}_1)$ and $p_2 = (E_2, \mathbf{p}_2)$ are the 4-momenta of the two colliding particles, and T is the temperature of the bath.[3] The above expression can be reduced to a one-dimensional integral which can be written in a Lorentz-invariant form as [16]

$$\langle\sigma v_{\text{Møl}}\rangle(T) = \frac{1}{8m_\chi^4 T K_2^2(m_\chi/T)}\int_{4m_\chi^2}^\infty ds\,\sigma(s)(s-4m_\chi^2)\sqrt{s}K_1\left(\frac{\sqrt{s}}{T}\right), \tag{2.6}$$

where $s = (p_1+p_2)^2$ is a usual Mandelstam variable and K_i denotes the modified Bessel function of order i.

[3]Note that in many cases one uses another definition of $< \sigma v_{\text{Møl}} >$ which involves a single thermal bath for both neutralinos. Compare, e.g., refs. [25, 34, 11].

In computing the cross section $\sigma(s)$, it is convenient to introduce a Lorentz-invariant function $w(s)$ [19]

$$w(s) = \frac{1}{4} \int d\,\mathrm{LIPS}\, |\mathcal{A}(\chi\chi \to \mathrm{all})|^2 \,, \tag{2.7}$$

where $|\mathcal{A}(\chi\chi \to \mathrm{all})|^2$ denotes the absolute square of the reduced matrix element for the annihilation of two χ particles, averaged over initial spins and summed over final spins. The function $w(s)$ is related to the annihilation cross section via [18]

$$w(s) = \frac{1}{2}\sqrt{s(s-4m_\chi^2)}\,\sigma(s)\,. \tag{2.8}$$

For a general annihilation process into a two-body final state $\chi\chi \to f_1 f_2$, the function $w(s)$ can be written as

$$w(s) = \frac{1}{32\,\pi} \sum \left[\theta\left(s-(m_{f_1}+m_{f_2})^2\right)\, \beta_f(s,m_{f_1},m_{f_2})\, \tilde{w}_{f_1 f_2}(s)\right], \tag{2.9}$$

where the summation goes over all possible channels, and

$$\tilde{w}_{f_1 f_2}(s) \equiv \frac{1}{8\pi} \int d\Omega\, |\mathcal{A}(\chi\chi \to f_1 f_2)|^2 \,, \tag{2.10}$$

where

$$\beta_f(s,m_{f_1},m_{f_2}) \equiv \left[1 - \frac{(m_{f_1}+m_{f_2})^2}{s}\right]^{1/2} \left[1 - \frac{(m_{f_1}-m_{f_2})^2}{s}\right]^{1/2} . \tag{2.11}$$

Computation of $w(s)$ is in general rather involved and final analytic expressions exhibit considerable complexity, as will be illustrated in the next section. This is one reason why in most of the literature one uses the well-known approximation in terms of expansion in powers of x, $\langle\sigma v_{\mathrm{Møl}}\rangle \simeq a + bx$. Using the definition (2.5), the expansion reads [19]

$$\langle\sigma v_{\mathrm{Møl}}\rangle = \frac{1}{m_\chi^2}\left[w - \frac{3}{2}(2w - w')\,x + \mathcal{O}(x^2)\right]_{s=4m_\chi^2} \equiv a + bx + \mathcal{O}(x^2) \tag{2.12}$$

where $w'(s)$ denotes $d\,w(s)/d\,(s/4m_\chi^2)$.

Note that in case of the expansion of $\langle\sigma v_{\mathrm{Møl}}\rangle$ defined in terms of a single thermal bath for both neutralinos, the corresponding coefficient a' is the same as eq. (2.12) while $b' = b + \frac{3}{2}a$ [30]. For more details, see, e.g., ref. [31].

The expansion method is widely used not only because it is computationally somewhat less involved but also because it is expected to be relatively accurate. This can seen by examining the behavior of the integrand in eq. (2.6). For a massive particle like the neutralino for which $T \lesssim m_\chi/20$ and $\sqrt{s} \geq 2m_\chi$, the argument of the function K_1 is much larger than unity. Since $K_1(y) \sim \sqrt{\pi/2y}e^{-y}$ at $y \gg 1$, the thermal average (2.6) can be written as a convolution of the cross section with a function $f(s)$:

$$\langle \sigma v_{\rm M\o l}\rangle \approx \int_{4m_\chi^2}^{\infty} ds\, \sigma(s) f(s)\,, \tag{2.13}$$

where $f(s)$ has an exponential suppression factor, $f(s) \propto e^{-\sqrt{s}/T}$. Thus one would expect that the usual expansion in powers of x should converge quickly [18].

One should however use this argument with some care. First, the annihilation cross section may change rapidly with s. It is well-known that this happens, e.g., near s-channel resonances and thresholds of new final states. In such cases the expansion method produces large errors [15]–[18]. Far away from such singular points the expansion is expected to give accurate results but, to our knowledge, this has never been explicitly verified in the literature. Finally, one would want to examine actually how far from resonances one can start relying on the usual approximation. As we will see later, the range of m_χ where the expansion fails to be reasonably accurate can be actually quite large.

3. Analytic results

As stated in the Introduction, we have derived a full set of exact, analytic expressions for the cross sections for the neutralino pair-annihilation processes into all allowed (tree-level) final states in the general MSSM. We have included all contributing diagrams as well as all interference terms and kept finite widths of all s-channel resonances. We have made no simplifying assumptions about sfermion masses although we assumed that there are no CP violating phases in SUSY parameters. Here we will give one analytic example of our exact expressions. A full set of results for all the final states will be given elsewhere [21].

Next, starting from the exact expressions we have computed the coefficients a and b using eq. (2.12) for all the partial annihilation channels. In the literature there exist several analytic formulae for the expansion coefficients, including [32, 33, 34, 11], but, due to different conventions and complexity of expressions, comparison is not always doable. We have checked our results for the a-coefficients in appropriate limits against published results and agreed in all cases. In the next section we will present a numerical comparison of the approximation in terms of the usual expansion with our exact results.

Let us begin by introducing the relevant MSSM parameters.[4] The lightest neutralino is a mass eigenstate given by a linear combination of two neutral gauginos and two neutral higgsinos

$$\chi = N_{11}\tilde{B} + N_{12}\tilde{W}_3 + N_{13}\tilde{H}_1^0 + N_{14}\tilde{H}_2^0\,. \tag{3.1}$$

The neutralino mass matrix is determined by the $\mathrm{U}(1)_Y$ and $\mathrm{SU}(2)_L$ gaugino mass parameters M_1 and M_2 (and we impose the usual GUT relation $M_1 = \frac{5}{3}\tan^2\theta_W M_2$),

[4]We follow the convention of ref. [35].

the Higgs/higgsino mass parameter μ and $\tan\beta = v_2/v_1$ which is the ratio of the vacuum expectation values of the two neutral Higgs fields.

There are two neutral scalar Higgs bosons h and H and one pseudoscalar A plus a pair of charged Higgs $H^\pm$. (We will typically suppress the Higgs charge assignment except where this may lead to ambiguities.) We use expressions given in ref. [36] for computing radiatively corrected Higgs masses.

Other relevant parameters which determine the masses of scalars and various couplings are the squark soft mass parameters m_Q, m_U and m_D, the slepton soft mass parameters m_L and m_E, and the pseudoscalar mass m_A. We also include the trilinear terms A_i $(i = t, b, \tau)$ of the third generation which are important in determining the masses and couplings for the stop, sbottom and stau sfermions, respectively.

There are a number of final states into which the neutralino can pair-annihilate. They include: $\chi\chi \to f\bar{f}$, WW, ZZ, Zh, ZH, ZA, $W^\pm H^\mp$, AA, AH, Ah, HH, Hh, hh and H^+H^-. Among these, in the gaugino region, fermion pair $f\bar{f}$ final states usually give dominant contributions, unless the exchanged sfermion masses $m_{\tilde{f}}$ are large and in some special cases, as discussed earlier. These final states are also always kinematically allowed (except for $t\bar{t}$) but, due to the s-wave suppression [9], their cross section is proportional to m_f^2/m_W^2. For the higgsino-like neutralinos the states ZZ and WW become very important once kinematically allowed [20]. However, these final states can give significant contributions even in the case of the gaugino-like neutralino. This is because WW and ZZ are not s-wave suppressed, unlike the channels hh, Hh, HH, AA, H^+H^- and ZA [11]. What is interesting is that the cross sections for the other s-wave unsuppressed states $W^\pm H^\mp$, Zh, ZH, Ah and AH, once kinematically allowed, can be even larger than those of WW and ZZ. In fact, they can even dominate over those of $f\bar{f}$. These points will be illustrated with numerical examples in section 4.

Here, we present a set of expressions for a t- and u-channel chargino exchange contribution to the process $\chi\chi \to W^+H^-$. (The two pairs of charginos are denoted by $\chi_i^\pm$ $(i = 1, 2)$ and $m_{\chi_i^\pm}$ represent their masses.) This contribution is often dominant. (There are also s-channel diagrams involving h, H and A exchange. Since typically $m_h \ll m_H \simeq m_A \simeq m_{H^\pm}$, the Higgs resonances will be outside of the kinematically allowed region.) The function $\tilde{w}$, eq. (2.10) in this case reads

$$\tilde{w}^{\chi^\pm}_{W^+H^-} = \frac{1}{m_W^2}\sum_{i,j=1}^{2}\left[m_{\chi_i^\pm} m_{\chi_j^\pm} I_{ij}^{(2)} + m_\chi m_{\chi_i^\pm} I_{ij}^{(1)} + I_{ij}^{(0)}\right], \tag{3.2}$$

where

$$\begin{aligned} I_{ij}^{(2)} = {} & (C_{+i}^{HW^*} C_{+j}^{HW} + D_{+i}^{HW^*} D_{+j}^{HW}) \times \\ & \times \left[-\mathcal{T}_2 - (s - m_W^2 - m_{H^\pm}^2 - 2\, m_\chi^2)\, \mathcal{T}_1 + G_{WH}^{T(1)}\, \mathcal{T}_0 + 6\, m_W^2 m_\chi^2\, \mathcal{Y}_0\right] + \\ & + (C_{+i}^{HW^*} C_{+j}^{HW} - D_{+i}^{HW^*} D_{+j}^{HW}) \left[6\, m_W^2 m_\chi^2\, \mathcal{T}_0 - \mathcal{Y}_2 + G_{WH}^{Y(1)}\, \mathcal{Y}_0\right], \end{aligned} \tag{3.3}$$

JHEP05(2001)063

$$
\begin{aligned}
I_{ij}^{(1)} &= \mathrm{Re}(C_{+i}^{HW^*} C_{-j}^{HW} + D_{+i}^{HW^*} D_{-j}^{HW}) \times \\
&\quad \times \Big[-2\mathcal{T}_2 + 2(2m_\chi^2 - m_W^2)\mathcal{T}_1 - 2(m_\chi^2 - m_W^2)(m_\chi^2 + 2m_W^2)\mathcal{T}_0 - \\
&\qquad - 3m_W^2 \mathcal{Y}_1 - G_{WH}^{Y(2)} \mathcal{Y}_0 \Big] + \\
&\quad + \mathrm{Re}(C_{+i}^{HW^*} C_{-j}^{HW} - D_{+i}^{HW^*} D_{-j}^{HW}) \Big[6\, m_W^2\, \mathcal{T}_1 + 6\, m_W^2 (m_\chi^2 - m_{H^\pm}^2)\mathcal{T}_0 - \\
&\qquad\qquad - 2\, \mathcal{Y}_2 (s - m_{H^\pm}^2 - 2\, m_W^2)\mathcal{Y}_1 - G_{WH}^{Y(3)}\, \mathcal{Y}_0 \Big],
\end{aligned} \tag{3.4}
$$

$$
\begin{aligned}
I_{ij}^{(0)} &= (C_{-i}^{HW^*} C_{-j}^{HW} + D_{-i}^{HW^*} D_{-j}^{HW}) \Big[(s - m_\chi^2 - 2\, m_W^2)\, \mathcal{T}_2 - G_{WH}^{T(2)}\, \mathcal{T}_1 \\
&\qquad - G_{WH}^{T(3)}\, \mathcal{T}_0 + (s - 2\, m_W^2)\, \mathcal{Y}_2 + G_{WH}^{Y(4)}\, \mathcal{Y}_0 \Big] + \\
&\quad + (C_{-i}^{HW^*} C_{-j}^{HW} - D_{-i}^{HW^*} D_{-j}^{HW}) \Big[6\, m_W^2 m_\chi^2\, \mathcal{T}_1 - m_\chi^2\, \mathcal{Y}_2 + G_{WH}^{Y(5)}\, \mathcal{Y}_0 \Big].
\end{aligned} \tag{3.5}
$$

Obviously the total contribution to $w(s)$ from $W^\pm H^\mp$ is twice that from W^+H^-. The symbols $C_{\pm i}^{HW}$ and $D_{\pm i}^{HW}$ in the above equations are combinations of several coupling constants:

$$
\begin{aligned}
C_{\pm i}^{HW} &\equiv C_S^{\chi_i^+\chi H^-} C_V^{\chi_i^+\chi W^{-*}} \pm C_P^{\chi_i^+\chi H^-} C_A^{\chi_i^+\chi W^{-*}}, \\
D_{\pm i}^{HW} &\equiv C_S^{\chi_i^+\chi H^-} C_A^{\chi_i^+\chi W^{-*}} \pm C_P^{\chi_i^+\chi H^-} C_V^{\chi_i^+\chi W^{-*}}.
\end{aligned} \tag{3.6}
$$

The relevant couplings describe neutralino-chargino-W^-/H^- interaction terms in the Lagrangian as

$$
\begin{aligned}
\mathcal{L}_{\rm int} &= \sum_{i=1}^{2} \overline{\chi_i^-} \gamma^\mu \left(C_V^{\chi_i^+\chi W^-} - C_A^{\chi_i^+\chi W^-} \gamma_5 \right) \chi W_\mu^- + \\
&\quad + \sum_{i=1}^{2} \overline{\chi_i^-} \left(C_S^{\chi_i^+\chi H^-} - C_P^{\chi_i^+\chi H^-} \gamma_5 \right) \chi H^- + \text{h.c.}
\end{aligned} \tag{3.7}
$$

in the convention of ref. [35]. The functions $\mathcal{T}_k = \mathcal{T}_k(s, m_\chi^2, m_{H^\pm}^2, m_W^2, m_{\chi_i^\pm}^2, m_{\chi_j^\pm}^2)$, $\mathcal{Y}_k = \mathcal{Y}_k(s, m_\chi^2, m_{H^\pm}^2, m_W^2, m_{\chi_i^\pm}^2, m_{\chi_j^\pm}^2)$, $k = 0, 1, 2$, and the functions $G_{WH}^{T(1-3)}$, $G_{WH}^{Y(1-5)}$ are listed in the appendix.

4. Numerical results

In this section we will illustrate the points made above by presenting several numerical results. We will concentrate on the gaugino-like neutralino. We remind the reader that a nearly pure gaugino (bino) is the most natural choice for the CDM both in the MSSM [23] and in the CMSSM where in most cases the LSP comes out to be a nearly pure bino [17, 12, 13].

JHEP05(2001)063

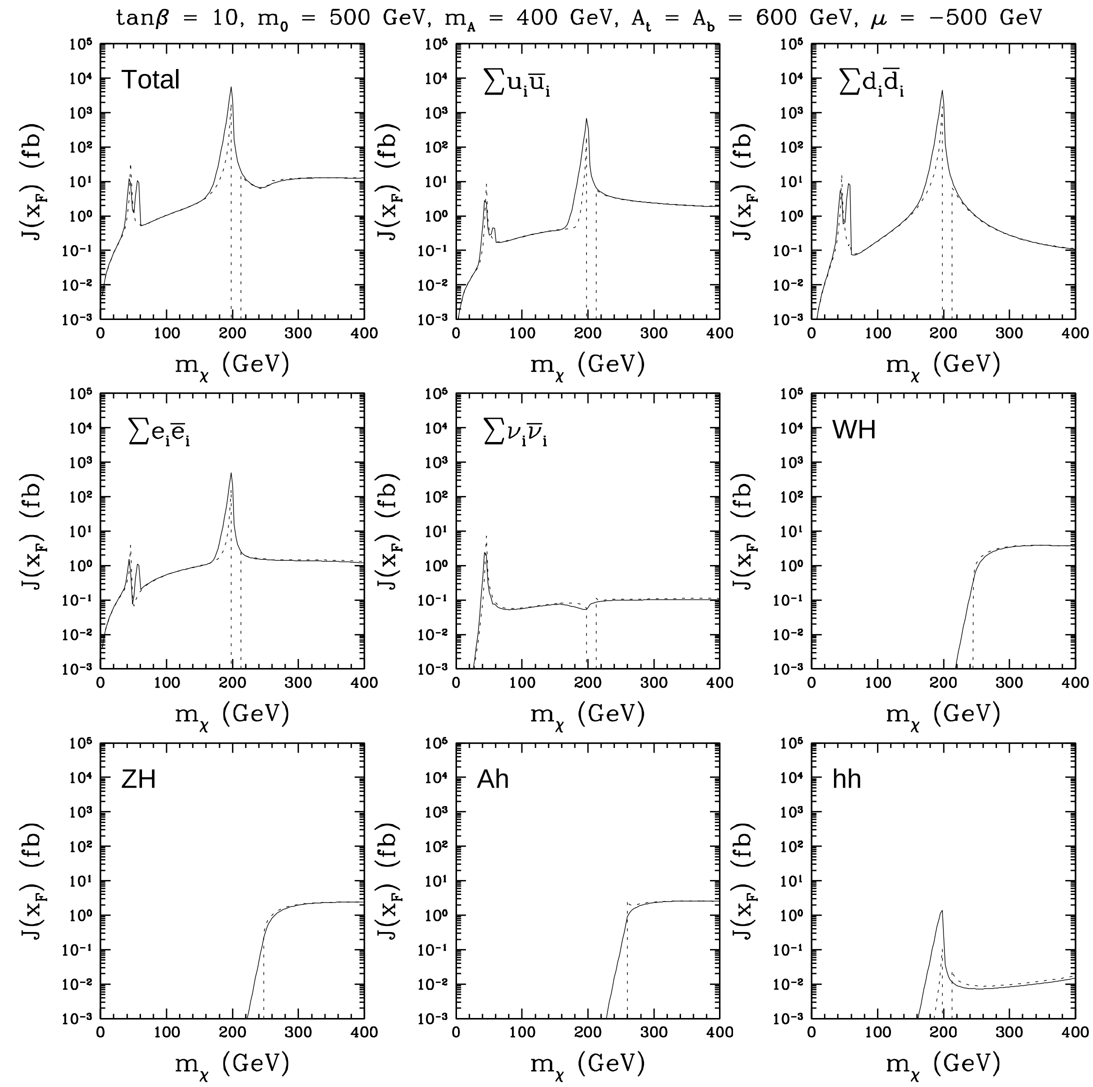

Figure 1: The total value of $J(x_f)$, eq. (2.4), and several partial contribution are shown in separate windows as a function of m_χ for $\tan\beta = 10$, $m_0 \equiv m_Q = m_U = m_D = m_L = m_E = 500\,\mathrm{GeV}$, $m_A = 400\,\mathrm{GeV}$, $A_t = A_b = 600\,\mathrm{GeV}$ and $\mu = -500\,\mathrm{GeV}$. The solid lines represent the exact results, while the dotted ones correspond to the expansion (2.12). Notice that the final states $W^\pm H^\mp$, ZH^0 and Ah, once kinematically allowed, give comparable contributions to the $f\bar{f}$ channels.

We begin by plotting in figures 1 and 2 the function $J(x_f)$, eq. (2.4), computed using exact and expansion methods as a function of m_χ. We take $\tan\beta = 10$, $m_0 \equiv m_Q = m_U = m_D = m_L = m_E = 500\,\mathrm{GeV}$, $m_A = 400\,\mathrm{GeV}$, $A_t = A_b = 600\,\mathrm{GeV}$ and $\mu = -500\,\mathrm{GeV}$. To obtain sparticle and Higgs mass spectra we have used the code DarkSusy. While several analytic expressions and numerical codes (e.g., SUSPECT [37]) are available in the literature, here we have used DarkSusy to facilitate the comparison of our results for the cross sections with those produced by the package. For the values given above we obtain the following Higgs masses: $m_h = 117.3\,\mathrm{GeV}$, $m_H = 400.5\,\mathrm{GeV}$ and $m_{H^\pm} = 407.9\,\mathrm{GeV}$.

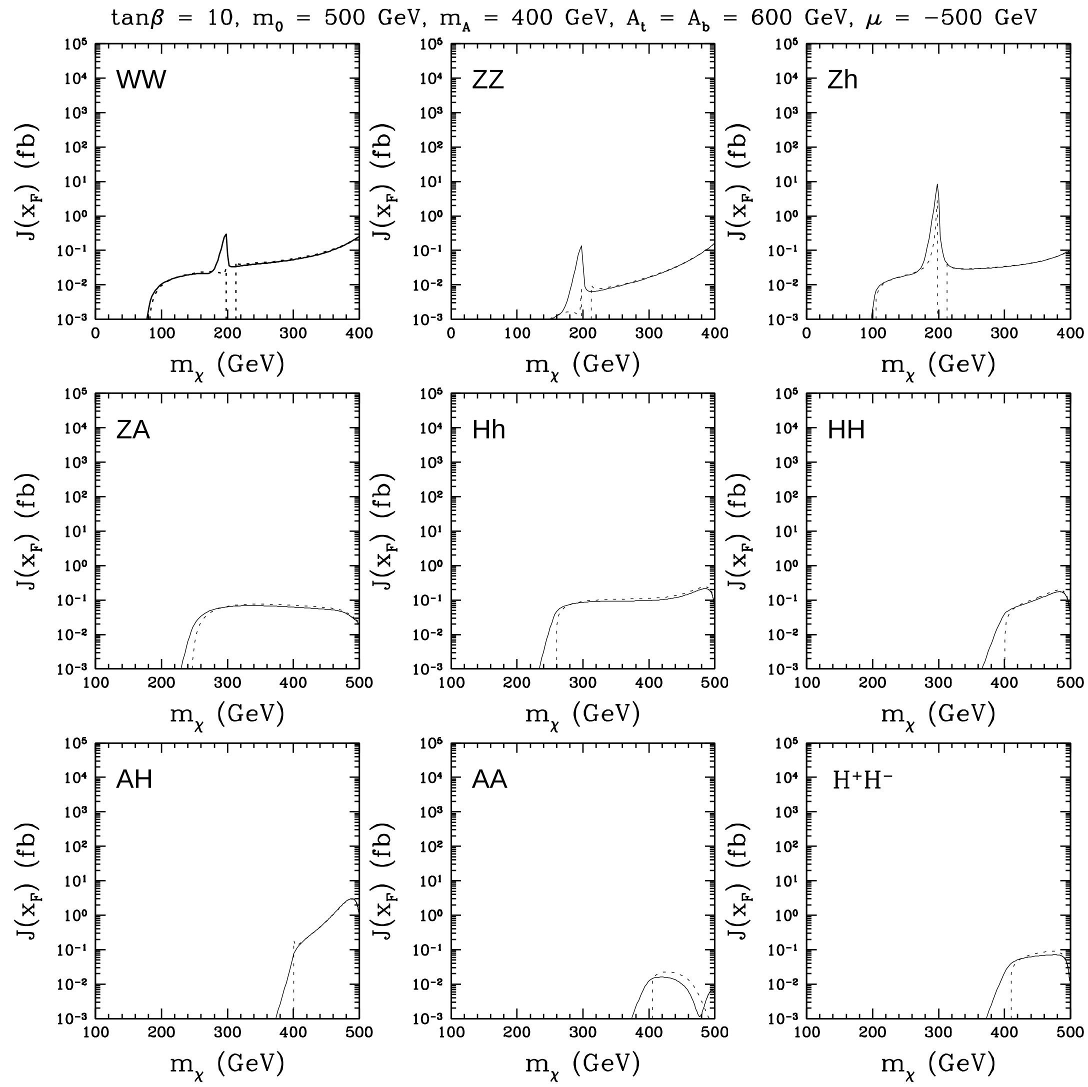

Figure 2: The same as in figure 1 but for mostly subdominant channels. Notice that in the lower two rows the horizontal axis has been shifted by 100 GeV.

We show both the total and the individual contributions from all the final states. The solid and dotted lines represent the exact and the expansion results, respectively. For the sake of comparison of both methods, for now we do not impose experimental constraints. Note that m_χ increases with increasing M_2 while we keep μ fixed at a rather large value. This means that in these figures (and also the following ones below), the neutralino is mostly a gaugino. Even at $m_\chi = 400\,\mathrm{GeV}$, $N_{11}^2 + N_{12}^2 > 0.9$. (However, between 400 GeV and 500 GeV the LSP turns into a nearly pure higgsino.) In this region the effect of co-annihilation with the lightest chargino and the next lightest neutralino, which we do not consider here, is not important and can be safely neglected.

For each final state, we compute $J(x_f)$, eq. (2.4), numerically via eq. (2.6) by using our exact expressions for the cross sections ($J_{\mathrm{exact}}(x_f)$). Next, we use the cross sections to compute the first two expansion coefficients a and b, as in eq. (2.12), and to compute $J_{\rm exp}(x_f) = ax_f + \frac{1}{2}bx_f^2$. For consistency, in both cases we determine the freeze-out point x_f by employing the iterative procedure (2.2). We will come back to the accuracy of the iterative procedure below.

In the behavior of the total $J(x_f)$ one can clearly recognize three peaks which are due to the s-channel Z, h and A/H exchange contributions. In particular, we can see that the A-resonance is very broad. (Due to a near mass degeneracy $m_H \simeq m_A$, the usually narrower H-pole is 'burried" underneath the A-pole.) This is caused by the amplification of the coupling $Ab\bar{b} \sim \tan\beta$ at larger $\tan\beta$ and the fact that, in the resonance region, the amplitude-square for the A-exchange is proportional to s, unlike the case of h and H where it goes like $s - 4m_\chi^2 \approx 0$ at $\sqrt{s} \approx 2m_\chi$. The Z-pole is also clearly visible in all the partial $f\bar{f}$ final states while the Higgs poles do not contribute to the $\nu\bar{\nu}$ final state since neutrinos do not couple to Higgs bosons. The H-pole also gives a visible enhancement to the WW, ZZ and hh final states but not to $W^\pm H^\mp$, ZA, HH, Hh, AA and H^+H^- which do not become kinematically allowed until $m_\chi > m_H/2$. Likewise, the A-pole shows a resonance in the Zh final state but not in $W^\pm H^\mp$, ZH, AH and Ah.

For the pseudoscalar Higgs exchange in $\chi\chi \to f\bar{f}$, the expansion method gives a discontinuity very close to the A-pole, $m_\chi \approx m_A/2 = 200\,\mathrm{GeV}$. For this channel, which is clearly dominant in the resonance region, the b-coefficient is large and negative and the expansion method and iterarative procedure break down. This can be clearly seen in all the $f\bar{f}$ windows (including $\nu\nu$) and also in the total value of $J_{\rm exp}(x_f)$. In the close vicinity of the poles, one can see the well-known large difference [15, 17, 18] (note a log scale) between $J_{\rm exact}(x_f)$ and $J_{\rm exp}(x_f)$ while away from the poles, both contributions are similar.

We can also notice that $J_{\rm exact}(x_f)$ and $J_{\rm exp}(x_f)$ show a significantly different enhancement in the total values and in the up-type quark-pair final state in the region $m_\chi \gtrsim m_t = 175\,\mathrm{GeV}$ where the $t\bar{t}$ final state becomes kinematically allowed. In particular, $J_{\rm exact}(x_f)$ increases gradually starting from m_χ some $10\,\mathrm{GeV}$ below m_t while $J_{\rm exp}(x_f)$ exhibits a sharp increase only at $m_\chi = m_t$. This is because the exact treatment takes into account the thermal distribution of momenta of the annihilating neutralinos, while the expansion method neglects it [15]. The same effect is visible near the thresholds of all the final states which only become open at some non-zero value of m_χ, especially of those involving one or two Higgs bosons.

As we stated in section 3, once kinematically allowed, the contributions from the $W^\pm H^\mp$ final state can be comparable, or even larger (if sfermion masses are increased) than the $f\bar{f}$ final state. In fact, the ZH, Ah and, at much larger m_χ also AH, final state contributions are not much smaller. We can also see that the channels ZZ and WW, as well as Zh, despite not being s-wave suppressed, are usually subdominant, except near $m_\chi \simeq m_A/2$ because of the pseudoscalar Higgs exchange contributing to those channels, and when the higgsino admixture of the neutralino increases which is the case with increasing m_χ while keeping μ fixed.

JHEP05(2001)063

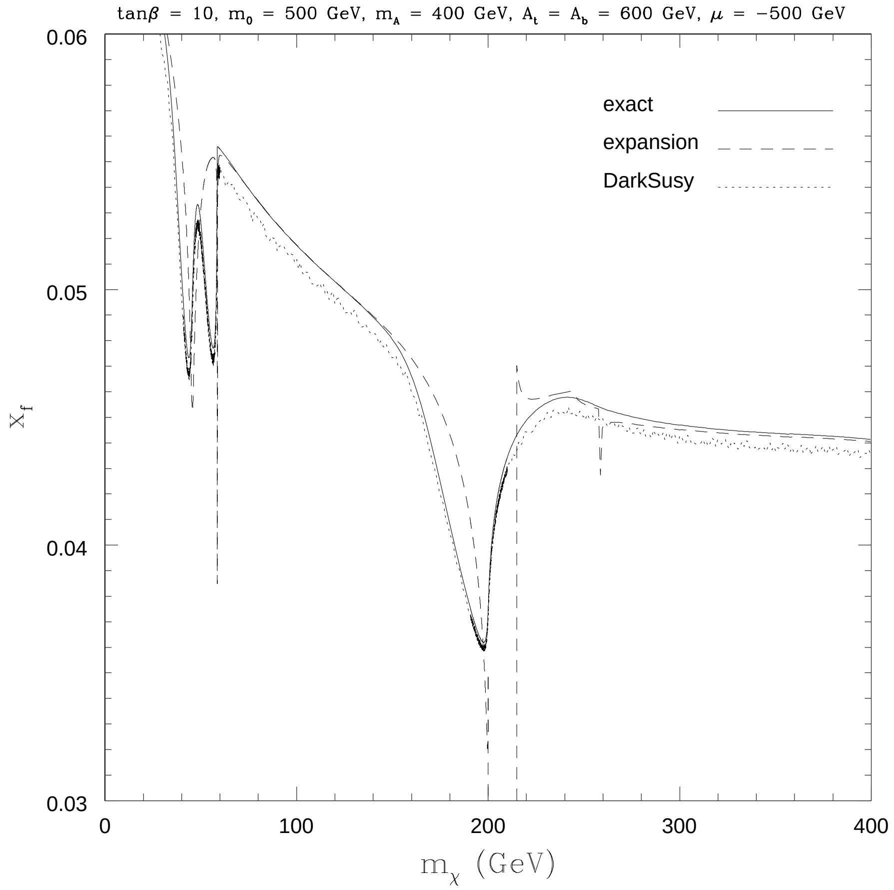

Figure 3: The freeze-out point x_f as a function of m_χ. The solid and dashed lines corresponds to the iterative procedure (2.2) with $\langle \sigma v_{\text{Møl}} \rangle$ computed exactly (2.5) and in terms of the expansion (2.12), respectively. For comparison, the dotted line has been obtained using DarkSusy.

As a way of verifying our results, we have performed a numerical comparison of our exact results for the cross section (more precisely of the function $w(s)$) with the same quantity computed using DarkSusy. We have found an excellent agreement at the level of a few per cent for all the tree-level final states when we fixed the same values of input parameters. This gives us some confidence that the (highly complex) expressions that we have derived (and also those in DarkSusy), are correct.

As mentioned above, in the current version of our numerical code we have used the iterative method (2.2) which is widely used in the literature. We applied it to both the exact formula for $\langle \sigma v_{\text{Møl}} \rangle$, eq. (2.6), and to the usual approximation (2.12). The results are presented in figure 3 as a solid and dashed line, respectively. For comparison, we also display x_f using DarkSusy (dotted line) where a different numerical procedure is used. It is clear that there is a general agreement among the three different procedures and also that x_f can be only roughly approximated by the usually quoted value 0.05. Away from the resonances and thresholds the expansion method can be safely used in determining x_f while near such special points this is not the

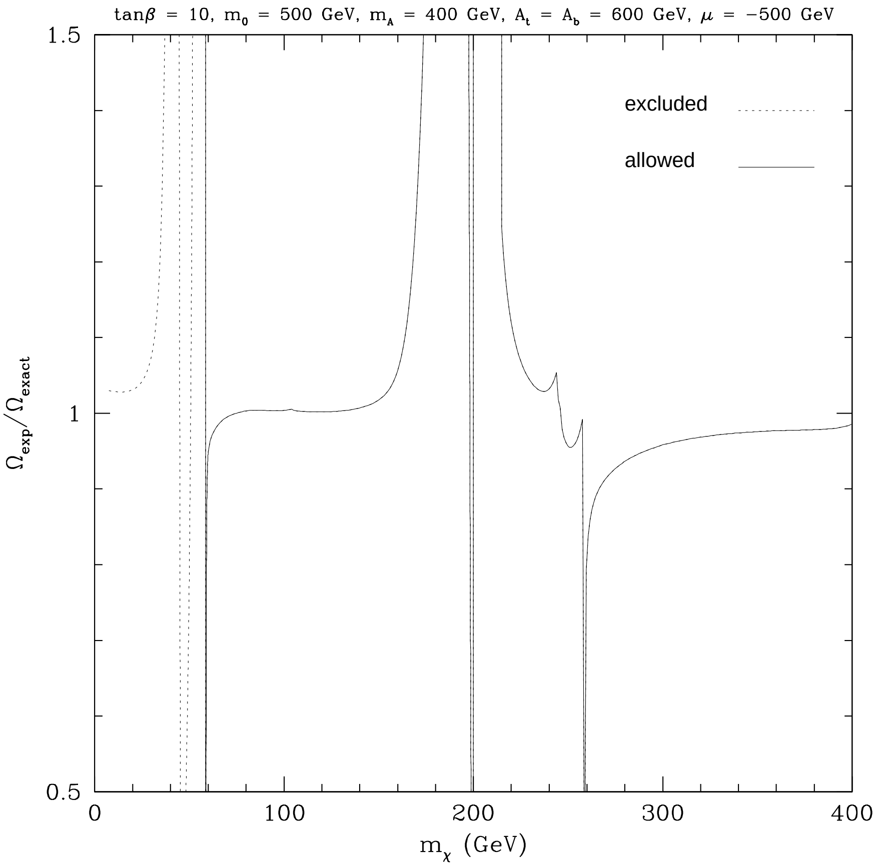

Figure 4: The ratio $\Omega_{\mathrm{exp}}/\Omega_{\mathrm{exact}}$ for the same choice of parameters as in figure 1. The solid (dotted) curves are allowed (excluded) by current experimental constraints. The relic aboundance is computed by solving eq. (2.2) iteratively and using eq. (2.3).

case. In particular, near the A-pole the expansion gives $\langle \sigma v_{\mathrm{Møl}} \rangle < 0$ and the iterative procedure breaks down. In contrast, the exact numerical integration (2.5) provides reliable results both near and away from special points. However, we have carefully verified that this is the case only when the integration in eq. (2.5) is performed with high enough numerical precision.

In figure 4, we plot the ratio $\Omega_{\mathrm{exp}}/\Omega_{\mathrm{exact}}$ versus m_χ for the same set of parameters as before. We denote by Ω_{exact} and Ω_{exp} the neutralino relic density calculated with the exact (2.6) and approximate (2.12) formulae for the thermal average, respectively. The relic abundance in both cases is computed by solving eq. (2.2) iteratively and using eq. (2.3). From now on we impose all applicable experimental constraints, including the lightest Higgs mass constraint $m_h > 113.5\,\mathrm{GeV}$ [38] and a lower bound $104\,\mathrm{GeV}$ for chargino masses. In the case of $b \to s\gamma$ we have followed DarkSusy in using a somewhat old range $1.0 \times 10^{-4} < B(b \to s\gamma) < 4.0 \times 10^{-4}$ [39] and have not yet included new SUSY contributions at large $\tan\beta$ that have been recently pointed out [40]. We feel that this is sufficient for the purpose of this analysis. The solid line represents the experimentally allowed region while the dotted line corresponds to the low m_χ range excluded by collider experiments.

JHEP05(2001)063

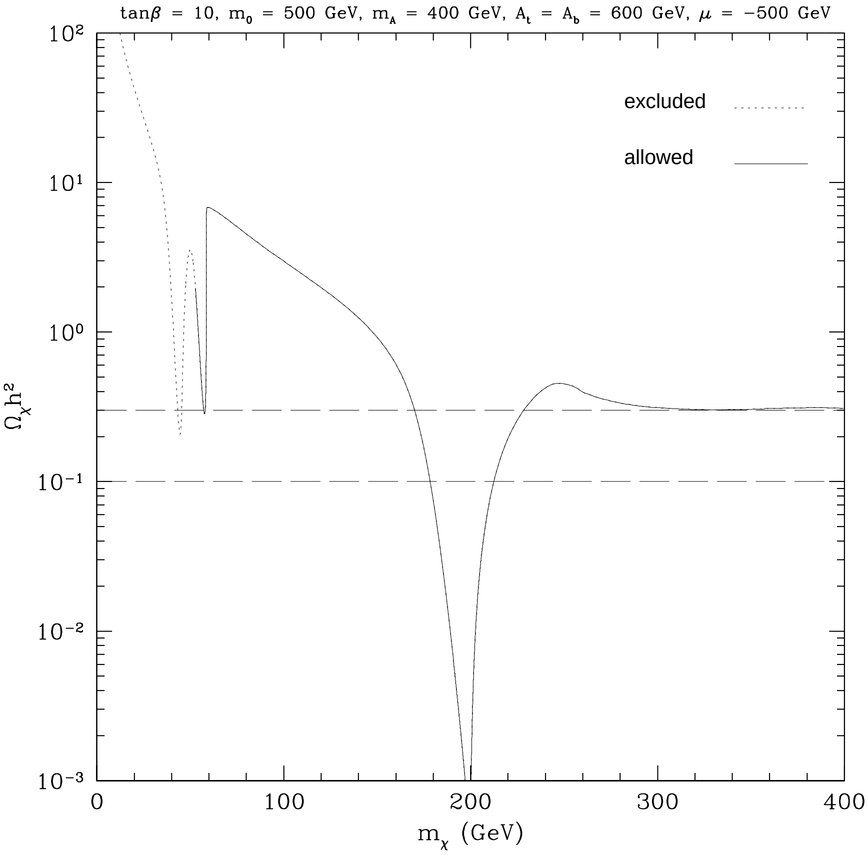

Figure 5: The relic density $\Omega_\chi h^2$ for the same choice of parameters as in figure 1. The solid (dotted) curves are allowed (excluded) by current experimental constraints. Here $\Omega_\chi h^2$ is computed using the exact expressions for the cross section. The band between the two horizontal dashed lines corresponds to the cosmologically favoured range $0.1 < \Omega_\chi h^2 < 0.3$.

It is evident that the ratio $\Omega_{\rm exp}/\Omega_{\rm exact}$ varies considerably with m_χ. Near resonances it is very large as discussed above. If we conservatively demand a 10% accuracy in the relic density computations then the approximate method fails to satisfy this criterion over a broad range $160\,\mathrm{GeV} \lesssim m_\chi \lesssim 220\,\mathrm{GeV}$, which is a significant fraction of the neutralino mass range. (In fact, various naturalness constraints, even if only indicative, give a rough constraint $m_\chi \lesssim 200\,\mathrm{GeV}$ [23, 24].) For larger values of $\tan\beta$ the range of m_χ where $0.9 < \Omega_{\rm exp}/\Omega_{\rm exact} < 1.1$ is not satisfied becomes even larger.

It is also clear that even further away from resonances the ratio $\Omega_{\rm exp}/\Omega_{\rm exact}$ exhibits a rather complex behavior. For $220\,\mathrm{GeV} \lesssim m_\chi \lesssim 260\,\mathrm{GeV}$ the new channels $W^\pm H^\mp$, ZA and ZH^0 successively kick in, and become actually even somewhat more important than $f\bar{f}$. Since, as we mentioned above, the expansion method does not work properly near new channels thresholds [15], the ratio varies quite rapidly over the mentioned range of m_χ, although not as much as near resonances. Finally, far away from resonances and thresholds, the expansion method seems to work remarkably well.

In figure 5 we show the relic abundance $\Omega_\chi h^2$ as a function of m_χ. Again, the solid (dotted) line represents the range of m_χ allowed (excluded) by the experimental constraints. The two horizontal dashed lines delimit the cosmologically expected range (1.1) of $\Omega_\chi h^2$. Two features should be mentioned. Over the range of smaller m_χ, in particular near resonances, the relic abundance varies rapidly. On the other hand, at larger m_χ, where new channels involving the "heavy" Higgs bosons $H^\pm$, A and H open up and can become important, $\Omega_\chi h^2$ exhibits a wide plateau. In both regions it is clearly important to compute $\Omega_\chi h^2$ accurately if one wants to achieve the accuracy expected from future determinations of $\Omega_{\rm CDM} h^2$. In particular, it is clear from figure 5 that at larger m_χ a relatively small difference of a few per cent in determining $\Omega_\chi h^2$ could allow on cosmological grounds the range of $m_\chi \gtrsim 320\,\mathrm{GeV}$ which in figure 5 is (barely) excluded. This again illustrates the need for reducing uncertainties involved in computing $\Omega_\chi h^2$ and in determining the cosmologically allowed regions of SUSY parameters.

5. Conclusions

While we are certainly still some time away from a "precision era" for measuring cosmological parameters, much effort has been focussed on improving theoretical calculations of the relic abundance of the neutralino. We have derived a full set of analytic expressions for the neutralino annihilation cross sections into all tree-level final states. In this paper, we have presented one example of such an expression for the neutralino annihilation into W^+H^- which can be even dominant. We have also computed the first two terms in the expansion of the exact formulae in powers of x and we have compared the integral of the thermally averaged product of the cross section and velocity and the relic abundance computed both ways. We have confirmed the well-known inaccuracy of the approximate method near reasonances and threshold and showed that, far away from such cases the expansion method works well. However, due to the presence of several resonances and thresholds in the MSSM, the expansion method may lead to sizeable errors over a relatively large range of the neutralino mass of up to several tens of GeV. We have also demonstrated that the iterative way of computing the freeze-out point works rather well for both the exact and expansion methods of computing the thermal average but not in the latter case near resonances and thresholds.

Acknowledgments

T.N. is grateful to the CERN Theory Division for its kind hospitality. L.R. would like to thank Mihoko Nojiri for helpful remarks.

A. Auxiliary formulae

Here we give expressions for the auxiliary functions used in the text. First, we define

$$D(s,x,y_1,y_2) \equiv x + \frac{y_1+y_2}{2} - \frac{s}{2}\,,$$
$$F(s,x,y_1,y_2) \equiv \frac{1}{2}\sqrt{s-4\,x}\sqrt{s-(\sqrt{y_1}+\sqrt{y_2})^2}\,\sqrt{1-\frac{(\sqrt{y_1}-\sqrt{y_2})^2}{s}}\,. \quad \text{(A.1)}$$

If we define $D \equiv D(s,x,y_1,y_2)$, $F \equiv F(s,x,y_1,y_2)$, $t_\pm(s,x,y_1,y_2) \equiv D \pm F$ and $(\mathcal{T}_i,\mathcal{Y}_i) \equiv (\mathcal{T}_i,\mathcal{Y}_i)(s,x,y_1,y_2,z_1,z_2)$ $(i=0,1,2)$, then

$$\mathcal{F}(s,x,y_1,y_2,z) = \frac{1}{2\,F}\,\ln\left|\frac{t_+(s,x,y_1,y_2)-z}{t_-(s,x,y_1,y_2)-z}\right|\,, \quad \text{(A.2)}$$

and

$$\begin{aligned}
\mathcal{T}_0 &= \frac{1}{z_1-z_2}\left[\mathcal{F}(s,x,y_1,y_2,z_1)-\mathcal{F}(s,x,y_1,y_2,z_2)\right],\\
\mathcal{T}_1 &= \frac{1}{z_1-z_2}\left[z_1\,\mathcal{F}(s,x,y_1,y_2,z_1)-z_2\,\mathcal{F}(s,x,y_1,y_2,z_2)\right],\\
\mathcal{T}_2 &= 1+\frac{1}{z_1-z_2}\left[z_1^2\,\mathcal{F}(s,x,y_1,y_2,z_1)-z_2^2\,\mathcal{F}(s,x,y_1,y_2,z_2)\right],\\
\mathcal{Y}_0 &= \frac{1}{z_1+z_2-2D}\left[\mathcal{F}(s,x,y_1,y_2,z_1)+\mathcal{F}(s,x,y_1,y_2,z_2)\right],\\
\mathcal{Y}_1 &= \frac{1}{z_1+z_2-2D}\left[2(z_1-D)\mathcal{F}(s,x,y_1,y_2,z_1)-2(z_2-D)\mathcal{F}(s,x,y_1,y_2,z_2)\right],\\
\mathcal{Y}_2 &= 1+\frac{1}{z_1+z_2-2D}\left[z_1(z_1-2D)\mathcal{F}(s,x,y_1,y_2,z_1)+z_2(z_2-2D)\mathcal{F}(s,x,y_1,y_2,z_2)\right].
\end{aligned}$$

The expressions for $G_{WH}^{T(i)}$ and $G_{WH}^{Y(j)}$, where $i=1,2,3$ and $j=1,\cdots,5$, in eqs. (3.3-3.5) are given by

$$\begin{aligned}
G_{WH}^{T(1)} &\equiv s(m_\chi^2+2m_W^2)-m_\chi^4-m_\chi^2(m_{H^\pm}^2+3m_W^2)-m_W^2m_{H^\pm}^2\,,\\
G_{WH}^{T(2)} &\equiv s(m_\chi^2+2m_W^2)-2m_\chi^4+m_\chi^2(m_{H^\pm}^2-m_W^2)-2m_W^2(m_{H^\pm}^2+m_W^2)\,,\\
G_{WH}^{T(3)} &\equiv (m_\chi^2-m_{H^\pm}^2)\,(m_\chi^2-m_W^2)\,(m_\chi^2+2\,m_W^2)\,,\\
G_{WH}^{Y(1)} &\equiv G_{WH}^{T(1)}\,,\\
G_{WH}^{Y(2)} &\equiv 3\,s\,m_W^2-12\,m_W^2m_\chi^2+3\,m_W^2m_{H^\pm}^2-3\,m_W^4,\\
G_{WH}^{Y(3)} &\equiv s^2-s(2m_\chi^2+2m_{H^\pm}^2+3m_W^2)+2m_\chi^4+(2m_\chi^2+m_{H^\pm}^2)(m_{H^\pm}^2+3m_W^2)-2m_W^4\,,\\
G_{WH}^{Y(4)} &\equiv s\,(m_\chi^2-2m_W^2)(m_\chi^2-m_{H^\pm}^2)+4m_W^2m_\chi^4+\\
&\quad +m_\chi^2(m_{H^\pm}^4-5m_W^2m_{H^\pm}^2+2m_W^4)-2m_W^4m_{H^\pm}^2\,,\\
G_{WH}^{Y(5)} &\equiv s\,m_\chi^2(m_\chi^2-m_W^2)-m_\chi^6-m_\chi^4(m_{H^\pm}^2+3m_W^2)+m_\chi^2m_W^2(2m_{H^\pm}^2+3m_W^2)\,.
\end{aligned}$$

References

[1] W.L. Freedman, *The Hubble constant and the expansion age of the universe*, *Phys. Rep.* **333** (2000) 13 [astro-ph/9909076].

[2] See, e.g., J.M. O'Meara et al., *The deuterium to hydrogen abundance ratio towards a fourth QSO: HS0105+1619*, astro-ph/0011179.

[3] P. de Bernardis et al., *A flat Universe from high-resolution maps of the cosmic microwave background radiation*, *Nature* **404** (2000) 955.

[4] A. Balbi et al., *Constraints on cosmological parameters from maxima-1*, *Astrophys. J.* **545** (2000) L1 [astro-ph/0005124].

[5] M.S. Turner and J.A. Tyson, *Cosmology at the millennium*, *Rev. Mod. Phys.* **71** (1999) S145 [astro-ph/9901113].

[6] For a review see, for instance, H.P. Nilles, *Supersymmetry, supergravity and particle physics*, *Phys. Rep.* **110** (1984) 1.

[7] H. Pagels and J.R. Primack, *Supersymmetry, cosmology and new TeV physics*, *Phys. Rev. Lett.* **48** (1982) 223;
S. Weinberg, *Cosmological constraints on the scale of supersymmetry breaking*, *Phys. Rev. Lett.* **48** (1982) 1303;
J. Ellis, J.E. Kim and D.V. Nanopoulos, *Cosmological gravitino regeneration and decay*, *Phys. Lett.* **B 145** (1984) 181.

[8] L. Covi, J.E. Kim and L. Roszkowski, *Axinos as cold dark matter*, *Phys. Rev. Lett.* **82** (1999) 4180 [hep-ph/9905212];
L. Covi, H.-B. Kim, J.E. Kim and L. Roszkowski, *Axinos as dark matter*, *J. High Energy Phys.* **05** (2001) 033 [hep-ph/0101009].

[9] H. Goldberg, *Constraint on the photino mass from cosmology*, *Phys. Rev. Lett.* **50** (1983) 1419.

[10] J. Ellis, J.S. Hagelin, D.V. Nanopoulos, K. Olive and M. Srednicki, *Supersymmetric relics from the big bang*, *Nucl. Phys.* **B 238** (1984) 453.

[11] G. Jungman, M. Kamionkowski and K. Griest, *Supersymmetric dark matter*, *Phys. Rep.* **267** (1996) 195 [hep-ph/9506380].

[12] R.G. Roberts and L. Roszkowski, *Implications for minimal supersymmetry from grand unification and the neutrino relic abundance*, *Phys. Lett.* **B 309** (1993) 329 [hep-ph/9301267].

[13] G.L. Kane, C. Kolda, L. Roszkowski and J.D. Wells, *Study of constrained minimal supersymmetry*, *Phys. Rev.* **D 49** (1994) 6173 [hep-ph/9312272].

[14] For a very recent analysis, see J. Ellis, T. Falk, G. Ganis, K.A. Olive and M. Srednicki, *The cmssm parameter space at large* $\tan\beta$, hep-ph/0102098.

[15] K. Griest and D. Seckel, *Three exceptions in the calculation of relic abundances*, *Phys. Rev.* **D 43** (1991) 3191.

[16] P. Gondolo and G. Gelmini, *Cosmic abundances of stable particles: improved analysis*, *Nucl. Phys.* **B 360** (1991) 145.

[17] P. Nath and R. Arnowitt, *Predictions in* SU(5) *supergravity grand unification with proton stability and relic density constraints*, *Phys. Rev. Lett.* **70** (1993) 3696 [hep-ph/9302318].

[18] J.L. Lopez, D.V. Nanopoulos and K. jia Yuan, *Accurate neutralino relic density computations in supergravity models*, *Phys. Rev.* **D 48** (1993) 2766 [hep-ph/9304216].

[19] M. Srednicki, R. Watkins and K.A. Olive, *Calculations of relic densities in the early universe*, *Nucl. Phys.* **B 310** (1988) 693.

[20] K. Griest, M. Kamionkowski and M.S. Turner, *Supersymmetric dark matter above the w mass*, *Phys. Rev.* **D 41** (1990) 3565.

[21] T. Nihei, L. Roszkowski and R. Ruiz de Austri, in preparation.

[22] P. Gondolo, J. Edsjo, L. Bergstrom, P. Ullio and E.A. Baltz, *DarkSUSY: a numerical package for dark matter calculations in the MSSM*, astro-ph/0012234;
The code DarkSUSY is available from http://www.physto.se/~edsjo/darksusy.

[23] L. Roszkowski, *Light neutralino as dark matter*, *Phys. Lett.* **B 262** (1991) 59.

[24] S. Dimopoulos and G.F. Giudice, *Naturalness constraints in supersymmetric theories with nonuniversal soft terms*, *Phys. Lett.* **B 357** (1995) 573 [hep-ph/9507282].

[25] E.W. Kolb and M.S. Turner, *The early universe*, Addison-Wesley 1990.

[26] S. Mizuta and M. Yamaguchi, *Coannihilation effects and relic abundance of higgsino dominant* lsp_s, *Phys. Lett.* **B 298** (1993) 120 [hep-ph/9208251].

[27] J. Edsjö and P. Gondolo, *Neutralino relic density including coannihilations*, *Phys. Rev.* **D 56** (1997) 1879 [hep-ph/9704361].

[28] J. Ellis, T. Falk, K.A. Olive and M. Srednicki, *Calculations of neutralino-stau coannihilation channels and the cosmologically relevant region of MSSM parameter space*, *Astropart. Phys.* **13** (2000) 181.

[29] K.A. Olive, D.N. Schramm and G. Steigman, *Limits on new superweakly interacting particles from primordial nucleosynthesis*, *Nucl. Phys.* **B 180** (1981) 497 [hep-ph/9905481].

[30] M. Srednicki, private communication, 1994.

[31] L. Roszkowski, *A simple way of calculating cosmological relic density*, *Phys. Rev.* **D 50** (1994) 4842 [hep-ph/9404227].

[32] J. Ellis, L. Roszkowski and Z. Lalak, *Higgs effects on the relic supersymmetric particle density*, *Phys. Lett.* **B 245** (1990) 545.

[33] K.A. Olive and M. Srednicki, *Cosmological limits on massive LSP's*, *Nucl. Phys.* **B 355** (1991) 208.

[34] M. Drees and M.M. Nojiri, *The neutralino relic density in minimal $N = 1$ supergravity*, *Phys. Rev.* **D 47** (1993) 376 [hep-ph/9207234].

[35] H.E. Haber and G.L. Kane, *The search for supersymmetry: probing physics beyond the standard model*, *Phys. Rep.* **117** (1985) 75;
J.F. Gunion and H.E. Haber, *Higgs bosons in supersymmetric models, 1*, *Nucl. Phys.* **B 272** (1986) 1.

[36] S. Heinemeyer, W. Hollik and G. Weiglein, *The mass of the lightest MSSM Higgs boson: a compact analytical expression at the two-loop level*, *Phys. Lett.* **B 455** (1999) 179 [hep-ph/9903404].

[37] A. Djouadi, J.-L. Kneur and G. Moultaka, The package SUSPECT is available at http://www.lpm.univ-montp2.fr:7082/~kneur/suspect.html.

[38] See, e.g., P. Igo-Kemenes, http://lephiggs.web.cern.ch/LEPHIGGS/talks/index.html.

[39] CLEO collaboration, *First measurement of the rate for the inclusive radiative penguin decay $B \to s\gamma$*, *Phys. Rev. Lett.* **74** (1995) 2885.

[40] G. Degrassi, P. Gambino and G.F. Giudice, *$B \to X_s$ gamma in supersymmetry: large contributions beyond the leading order*, *J. High Energy Phys.* **12** (2000) 009 [hep-ph/0009337];
M. Carena, D. Garcia, U. Nierste and C.E.M. Wagner, *$B \to s\gamma$ and supersymmetry with large* $\tan\beta$, *Phys. Lett.* **B 499** (2001) 141 [hep-ph/0010003].